

Calculating the Segmented Helix Formed by Repetitions of Identical Subunits

Robert L. Read¹

Public Invention, Austin, TX 78704, USA,
read.robert@gmail.com,
WWW home page: <https://www.pubinv.org>

Abstract. Eric Lord has observed:

In nature, helical structures arise when identical structural subunits combine sequentially, the orientational and translational relation between each unit and its predecessor remaining constant.[1]

If a robot is composed of modular structural subunits can change their shape, the shape of the robot can change. If they all change in the same way, the robot will be a segmented helix of varying length. Constant-time algorithms consisting of analytic expressions are given for the segmented helix generated from the intrinsic properties of a stacked object and its conjoining rule. The construction of these from the intrinsic properties of the rule for conjoining repeated subunits of arbitrary shape is provided, allowing the complete parameters describing the unique segmented helix generated by arbitrary stackings to be easily calculated. Free-libre open-source interactive software and a website[4] is provided which performs this computation for arbitrary prisms along with interactive 3D visualization[5]. This allows the deduction of intrinsic properties of a repeated subunit from known properties of a segmented helix, as a chemist might want to do. Because the algorithms are efficient, a repeated subunit can be designed to create a segmented helix of desired properties, as a mechanical engineer or roboticist might want. A theorem, proved in [14] is provided that any subunit can produce a toroid-like helix or a maximally-extended helix, forming a continuous spectrum based on joint-face normal twist. As a verification and demonstration, the software, website and paper compute, render, and catalog an exhaustive “zoo” of 28 uniquely-shaped platonic helices, such as Boerdijk-Coxeter tetrahelix and various species of helices formed from dodecahedra.

Keywords: Helix, Variable Geometry Truss, Segmented Helix, Solid Geometry, Screw Theory, Platonic Helix

Mathematics Subject Classification: 97G40, 52B12

1 Introduction

During the Public Invention Mathathon of 2018[6], software was created to view chains of regular tetrahedra joined face-to-face. The participants noticed whenever the rules defining the face to which to add the next tetrahedron were periodic, the resulting structure was always like a discrete helix.

Although unknown at that time, this is a consequence of:

Observation 1 (Lord’s Observation) *In nature, helical structures arise when identical structural subunits combine sequentially, the orientational and translational relation between each unit and its predecessor remaining constant.[1]*

Although fairly obvious in hindsight from screw theory, we have found no articulation of this statement in writing, so feel justified in naming it after the author of its earliest statement. The surprising fact that DNA is a double helix allows replication and RNA synthesis by the unzipping and rezipping of the helix. However, the fact that it is helical in nature is unsurprising, since it follows directly from Observation1 and the fact that the strands DNA are formed of repeated chemical units of approximately the same shape arranged sequentially. The purpose of this paper is to provide mathematical tools and software for studying arbitrary segmented helices generated in this way. A proof of Lord's Observation is provided in a longer version [14].

Finding the properties of a segmented helix from three contiguous segments on the helix from screw theory[2,3], is explained and formulated. An interactive, 3D rendering website written in JavaScript which allows both calculation and interactive play and study is provided[5] (see Figure 2). This allows a structure, or "molecule", coincident to a segmented helix to be designed by adjustments to the repeated object, or for the shape of a repeated subunit to be inferred from the intrinsic properties of the segmented helix. Kahn's method of helix fitting[3,7,8] is modified to cover some degenerate situations.

We exploit Lord's Observation to discover symmetry which allows us to compute the helix when subunits are joined face-to-face with the same *twist*. Kahn was investigating proteins, which do not have faces, but geometric solids and other macroscopic solid objects do. This concept can be generalized to a *joint face angle*, even if the objects conjoined do not technically have flat faces. This symmetry allows us to compute the parameters of the segmented helix purely from properties intrinsic to a single object and the joining rule. We prove that varying the *twist* of the joint faces through a complete rotation produces a smoothly varying spectrum of shapes that always includes a torus-like shape and a *zig-zag* planar segmented helix of maximal extent. A robot thus constructed of identical modules, such as the TetRobot of 1 which can change their shape allows the helix to coil and uncoil predictably based on the math herein.

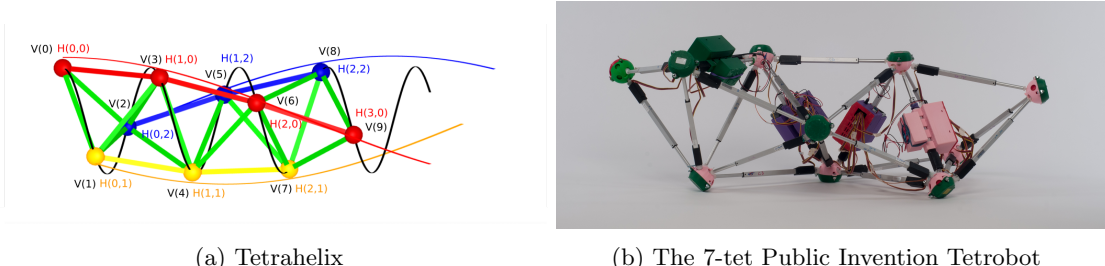


Fig. 1: Tetrahelix Robots

2 The Segmented Helix

A goal is to derive the parameters for a continuous helix from such discrete objects by studying a helix evaluated at integral points. Call such an object a *segmented helix*. A segmented helix

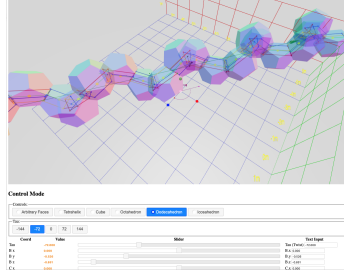


Fig. 2: Example Segmented Helix Generated From the Dodecahedron

may be thought of as function that, given an integer, gives back a point in 3-space.

$$P_x(n) = r \sin n\theta \quad (1)$$

$$P_y(n) = r \cos n\theta \quad (2)$$

$$P_z(n) = nd \quad (3)$$

d is the distance or *travel* along the helix axis between adjacent joints. In this canonical representation the helix axis is the z -axis. θ is the rotation around the z -axis between adjacent points. r is the radius of the segmented helix. Note that if $\theta = \pi$, a third form of degeneracy (to the human eye) occurs: that of a segmented helix which is a zig-zag contained completely within a single plane.

If one thinks of the segmented helix as describing a polyline in 3-space, the properties of that polyline are of interest. Considering only the *intrinsic* shape of the segmented helix that are independent of position and orientation in space, there are three degrees of freedom: r , d , and θ .

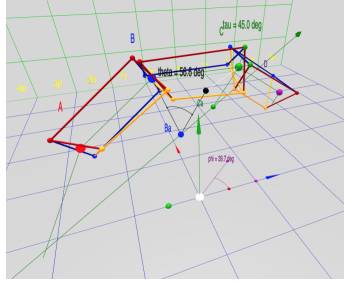


Fig. 3: Naming of measures

Figure 3 demonstrates naming convention concepts. It is a screen shot taken from the interactive website[5]. The software allows parallax by supporting interactive rotation, which makes the 3D structure easier to perceive; please visit the interactive page during this discussion of naming conventions.

In Figure 3 and the website, we represent the object as a prism with triangular cross-section, because this is the simplest physically realizable macroscopic object that supports a face-to-face connection. In this diagram, the points A , B , C , and D are represented by the sphere of

the same color as the label. The view is roughly in the direction of the axis of the segmented helix, which is drawn as a dark green arrow, pointing in the positive z and positive x direction, parallel to the XZ -plane. For ease of viewing, the entire segmented helix has been raised by two units on the y axis. The segment \overline{BC} has coordinate $y = 2$, is aligned with the z -axis, and centered in the z direction.

The positive x , y and z axes are shown by the red, green, and blue axis arrows, respectively. Following computer graphics convention, the y axis is oriented vertically. The points A , B , C , and D correspond to $P(0)$, $P(1)$, $P(2)$, and $P(3)$, respectively, for a segmented helix aligned to the raised axis (not the z -axis). A thin green polyline represents the segmented helix, and thus connects the joints A , B , C , and D . The points are wrapping around the axis clockwise, with an angle of $\theta = 56.6^\circ$ as shown by the on-screen protractor as the rotation from one point to the next. As will be explained in Section 6, τ is the face-on-face joint rotation, in this case of 45° . The helix angle $\phi = 39.7^\circ$ is rendered by a protractor on the $y = 0$ plane; this is the angle between the axis and of the helix and the z axis, and therefore the angle of any one segment against the helix axis.

Any point on the segmented helix has a closest point on the axis of the helix. In particular, the points closest to the joints are called *joint axis points*. Then d is the distance along the axis between consecutive joint axis points.

A line is drawn from the blue point B to a black sphere on the helix axis, the joint axis point, denoted B_a . Analogously, C_a is the point on the axis closest to the green point C .

A segmented helix located in space is completely determined by the parameters r, d, θ , a vector describing the axis of the helix, and the position of any one joint.

Because the segmented helix is a discrete structure, one can reframe the concept of *pitch* as *sidedness* s : how many segments (sides) make a complete rotation?

The following concepts and conventional variable names for them will be related:

- L is the distance between any two adjacent joints (between B and C , for example).
- r is the distance between a joint and the helix axis (between B and B_a for example).
- θ is the rotation about the helix axis between two consecutive joints.
- c is the length of a chord formed by the projection of the segment between two points projected along the axis of the segmented helix (a chemist may recognize this as the distance between residues on a *helical wheel* projection).
- d is the distance along the axis of the helix between any two joint axis points (between B_a and C_a in Figure 3, for example, rendered as a small black and blue sphere, respectively).
- ϕ is the angle between any vector between two adjacent joints and the axis of the helix. In physical screws used in mechanical engineering, this is analogous to the *helix angle*.
- p is the pitch of the helix, the distance traveled in one complete rotation.
- s is the number of segments in a complete rotation (in general not rational).
- Finally, we find it useful to define the *tightness* of a segmented helix as travel divided by radius, a number analogous to the extension of a coil spring or slinky. A torus-like segmented helix has zero tightness and a zig-zag has maximum tightness. The letter t represents tightness.

These quantities are related:

$$c = 2r \sin \frac{\theta}{2} \quad (4)$$

$$L^2 = c^2 + d^2 \quad (5)$$

$$\arctan \frac{c}{d} = \phi \quad (6)$$

$$s = \frac{2\pi}{\theta} \quad (7)$$

$$d = L \cos \phi \quad (8)$$

$$p = d \cdot s \quad (9)$$

$$t = d/r \quad (10)$$

Please see the longer version of this paper for a full discussion of some convenient conventions. Sections 5 and 6 relate these properties to properties intrinsic to the joint or interface between two segments or objects in the segmented helix.

3 The Intrinsic Properties of Periodic Chains of Solids

Although fairly obvious from Chasles' Theorem, in order to prove Observation 1, additional clarification is helpful. If chains of identical repeated 3D units are conjoined identically, they are *periodic chains*, and they generate a segmented helix coincident on their joints. Identical objects conjoined via a rule produce periodic chains of objects that are uniformly intersected by segmented helices and may be degenerate in one of three ways that might not strike the human eye as a helix at first glance:

1. The segments may form a straight line.
2. The segments may be planar about a center, forming a polygon or ring.
3. The segments may form a planar saw-tooth or zig-zag pattern of indefinite extent.

There are two complementary ways of learning about such segmented helices. In one approach, we may have knowledge of the segmented helix and wish to learn about the subunits and the rule with which the subunits are combined. In the other approach, one may know *a priori* exactly the relevant properties of the objects and the rule with which they combine and seek to compactly describe the segmented helix they create.

4 Periodic Chains Produce Segmented Helices

A periodic chain is, in fact, a simple object which demonstrates tremendous symmetry. Before using this symmetry in the construction of the segmented helix corresponding to a periodic chain, it is valuable to prove that such a segmented helix indeed exists for every periodic chain. Because periodic chains are merely a clarification of the “identical structural subunits” of Observation 1, this theorem proves that observation.

Theorem 1 (Segmented Helix). *Consider N identical objects which each have two points, A and B , called joints. Call \overrightarrow{AB} the axis of this object. Consider the frame of reference for this object to have its axis on the z -axis with B in the positive direction, the midpoint of the object being at the origin.*

Consider any rule that conjoins A of object $i+1$ to B such that from the frame of reference of i , the object $i+1$ and anything rigidly attached to it is always in the same position in the frame of reference for i . Informally, $i+1$ “looks the same” to i , no matter what i is chosen,

$i < N$. Call a chain of N identical rigid objects conjoined via a rule that conjoins A_{i+1} to B_i in such a way that every vector of B is always in the same position relative to a frame of reference constructed from A , a periodic chain.

Any periodic chain of three or more objects has a unique segmented helix whose segments correspond to the axes of these objects.

A proof is provided in the longer version of this paper[14].

Consider objects which are, taken as individuals, highly asymmetric. For example, the B face does not have to be the same size as the A face. In fact, the object itself might be shaped like the letter “C”, and not completely enclose the axis. Taking the idea further, the object might be spiky like a stellated polyhedron or a sea urchin, and still be joined by joints relatively close to the center of the object. (This paper does not address the issue of self-collision of the objects, which would have to be considered if attempting to make a period chain of sea urchins).

It is perhaps not obvious that building a chain of such objects produces a segmented helix, and therefore that the helix angle is the same for each object, but this is a corollary of Theorem 1.

5 PointAxis: Computing Segmented Helices from Joints

Kahn[3] has given a method for computing the axis of a helix in the context of chemistry. This method uses the observation that the angle bisectors of the segments on a segmented helix are perpendicular to and intersect the axis of the helix. Because chemical helices may not be perfect and because the measurement of positions may not be perfectly accurate, it is common for chemists to use regression and fitting methods to fit helix parameters to observed positions on the helix. Kahn’s method was a prelude to some error-tolerant methods applicable to the realm of organic chemistry[7]. This paper is concerned only with pure geometry. Also, Kahn was writing in 1989, and more convenient computing tools are now available. The algorithm presented, called *PointAxis*, here can be considered a modification of Kahn’s algorithm, which relies on the ability, working in the realm of pure geometry, to position the segments on the axes to simplify the derivation and computation.

5.1 A Sketch of the 4-Point Method

Using tools from linear algebra and well-documented algorithms, a sketch of finding the segmented helix from four consecutive known points A, B, C , and D is:

- Construct a rigid transformation that places the points conveniently on the z -axis and balanced around the y -axis.
- Compute the bisectors of the angle between object axes $\angle ABC$, called $\overrightarrow{B_b}$ and the bisecting angle $\overrightarrow{C_b}$ of $\angle BCD$. If the points are collinear, they are a special case.
- Because these angle bisectors point at the axis of the segmented helix, their cross product is a vector in the direction of the axis. If $\overrightarrow{B_b}$ and $\overrightarrow{C_b}$ are parallel or anti-parallel the cross product is not defined and we have special cases.
- Otherwise the vectors $\overrightarrow{B_b}$ and $\overrightarrow{C_b}$ are skew, and the algorithm for the closest points on two skew lines provides two axis points B_a and C_a on these vectors which are the closest points on those lines and are also points on the helix axis.
- The distance between B_a and B is the radius, and the distance between B_a and C_a is the travel d along the axis.
- The angle between $\overrightarrow{B - B_a}$ and $\overrightarrow{C - C_a}$ is θ .

5.2 Rotating into Balance from Face Normal Vectors

In order to use the *PointAxis* algorithm, we need a way to compute points A and D in balance around the axis BC .

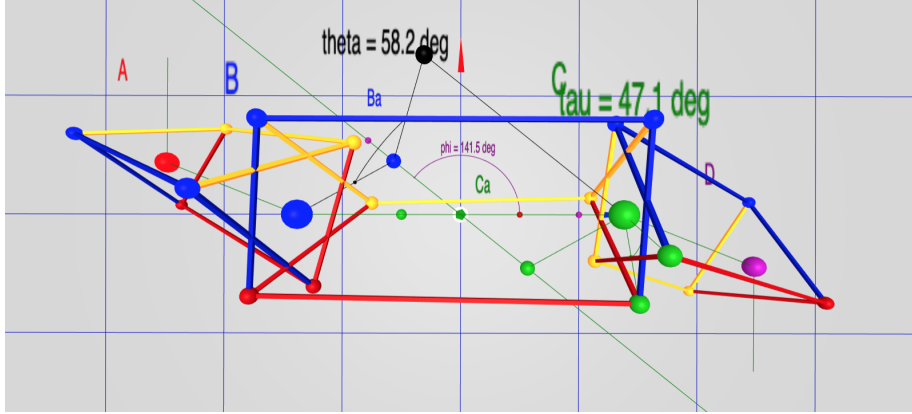


Fig. 4: A Balanced Configuration

Figure 4 shows a downward view of a balanced configuration (though raised above the origin instead of at the origin). A (the red sphere) is a reflection of D (the purple sphere) across the y -axis. Both A and D are hanging downward. If the structure were hung on a point at the origin, it would be physically balanced. As shown in the following, it is always possible to achieve this balance, even though a single object itself is not symmetric; in this figure the normal of the B face is not symmetric with C face.

That this is always possible is important enough, if only for the convenience of calculation, that we consider it a Lemma:

Lemma 1 (Balance Lemma). *For any segmented helix with selected consecutive joints A, B, C and D , there is a rigid transformation which positions it such that:*

- *The segment BC is centered on the z -axis: $(B_x = 0 \wedge B_y = 0 \wedge C_x = 0 \wedge C_y = 0) \wedge B_z < 0 \wedge C_z = -B_z$.*
- *The joints A and D are in rotational balance about the y axis, as if they were weights hanging downward: $A_y = D_y \wedge A_y \leq 0$ and $A_x = -D_x \wedge A_z = -D_z$.*

A proof sketch is provided in the longer version of this paper[14].

The screw axis may now be computed from either the four points A, B, C , and D or from the transformation matrix created to balance them.

5.3 The 4-Point Method

Four consecutive points completely determine at least one segmented helix. Consider only the helix that makes the least rotation between these points, though more rapidly rotating helices will also intersect these points. The *PointAxis* algorithm takes four such points. Without loss of generality B and C are assumed to be centered on the z -axis, and that a rotation has been performed to balance A and D so that $A_x = -D_x, A_z = -D_z$, and $A_y = D_y$. Thus the input

to *PointAxis* in fact has only three degrees of freedom, which determine the three intrinsic properties r, d, θ which completely define the shape of a segmented helix (but not its location in space).

In the derivations below, we rely on certain facts about the segmented helix formed by the stack of objects, the first of which is key:

- By virtue of Lemma 1, without loss of generality, think of any member whose faces and twist generate a non-degenerate helix as being “above” the axis of the helix. Furthermore choose to place the object in this figure so that $B_y = C_y$, that is, that the members are symmetric about the z -axis. A and D are “balanced” across the YZ -plane, and $A_x = -D_x$ and $A_y = D_y$.
- Every joint (A, B, C , and D) is the same distance r from the axis H of the helix.
- Every member is in the same angular relation ϕ to the axis of the helix.
- Since every member of a non-degenerate helix cuts across a cylinder around the axis, the midpoint of every member is the same distance from the axis which is, in general, a little a less than r . In particular the midpoint M whose closest point on the helix axis m is on the y -axis and $\|\overrightarrow{Mm}\| < \|\overrightarrow{B_b}\|$.
- The points (A_a, B_a, C_a, D_a) on the axis closest to the joints (A, B, C, D) are equidistant about the axis and centered about the y -axis. In particular, $\|\overrightarrow{B - B_a}\| = \|\overrightarrow{C - C_a}\|$.

From the observations that $\|\overrightarrow{B - B_a}\| = \|\overrightarrow{C - C_a}\|$ it becomes clear that the helix axis is in a plane parallel to the XZ -plane, it intersects the y -axis, but in general is not parallel to the z -axis.

Because the angle bisectors of each joint are in general skew, and intersect the axis perpendicularly, the algorithm for the closest points on two skew lines finds B_a and C_a .

However, a segmented helix has tremendous symmetry, and the angle bisectors are very far from being two generally skew lines. In fact, by taking advantage of the fact that the generating rule for an object chain requires similarity in every joint, the objects can be arranged as in Figures 3 and ??.

PointAxis takes a length and a point D known to be in a specific relation to B and C . This careful arrangement of the axes allows the computation of ϕ , the angle between the helical axis and the z axis. This, in combination with symmetry and the knowledge that the helical axis is in the XZ plane, supports computing the points on the axis corresponding to the joints directly from ϕ .

This algorithm coded below is simple enough that Mathematica[15] can actually produce a symbolic closed-form formula for all computed values in terms of L, x, y , and z . However, these formulae are less comprehensible to the human eye than this algorithm. Their existence does open the possibility that, for example, the derivative representing the change in r with a change in D could be calculated.

5.4 Degenerate Cases

Define the angle bisector vectors:

$$\overrightarrow{B_b} = B - (A + C)/2 \quad (11)$$

$$\overrightarrow{C_b} = C - (B + D)/2 \quad (12)$$

The fundamental insight that the axis of the helix H can be computed by a cross product of the angle bisector vectors ($\overrightarrow{B_b}$ and $\overrightarrow{C_b}$) applies only when the angle-bisectors have a non-zero length and when they are not anti-parallel. When they are of zero length, this is the degenerate case of a straight line coinciding with all segments. When $\overrightarrow{B_b}$ and $\overrightarrow{C_b}$ are parallel and pointing in opposite directions, the zig-zag degeneracy occurs. The math for both of these cases is provided in the longer paper[14].

5.5 Standard Case

However, the most general case is simpler and can be worked out with standard linear algebra operations. In the math below, which is a direct analog of our coded solution, the tremendous symmetry of the “balance” condition permits the computation to proceed with using mostly scalar operations. There is some hope that this would allow closed-form expressions to be produced, perhaps with the aid of a symbolic computation system such as Mathematica[15]. If completed, this would allow us to give closed-form solution to the intrinsic properties of all the 28 Platonic helices enumerated in Sec ??.

Once \vec{H} has been calculated, the signed travel along the axis d is the scalar projection of a segment $\overrightarrow{C-B}$ onto \vec{H} . From this ϕ is directly calculable. ϕ allows a direct calculation of the x, y and z components of the point B_a on the axis pointed to by \vec{B}_b . r is the distance between B_a and B . c and θ are easily computed from these values.

$$\vec{H} = \begin{bmatrix} -2B_{b[y]}B_{b[z]} \\ 0 \\ 2B_{b[y]}B_{b[x]} \end{bmatrix} \quad (13)$$

$$d = \frac{LB_{b[x]}}{\sqrt{B_{b[x]}^2 + B_{b[z]}^2}} \quad (14)$$

$$\phi = \text{atan2}(H_z, H_x) - \pi/2 \quad (15)$$

$$c = \sqrt{L^2 - d^2} \quad (16)$$

In this approach to calculation, it is easiest to compute the axis point B_a corresponding to B and use it to complete our computations.

From trigonometry and utilizing the facts that

$$\phi = \arccos(d/L) \quad (17)$$

$$\sin(\arccos x) = \sqrt{1 - x^2} \quad (18)$$

it can be shown that the x and z component of B_a are:

$$B_{a[x]} = \frac{d\sqrt{1 - (d/L)^2}}{2} \quad (19)$$

$$B_{a[z]} = -\frac{d^2}{2L} \quad (20)$$

However, this computation exposes another special case: when the helix angle ϕ is $\pi/2$, the segmented helix is torus-like. In this case the axis point B_a is in fact on the y -axis, and so only $B_{a[y]}$ is need:

$$B_{a[y]} = \frac{LB_{b[y]}}{2B_{b[z]}} \quad (21)$$

Except for in the toroidal case, $B_{b[x]}$ must be taken into account, but it is non-zero, so we can divide by it. By imagining a plane pressed downward from the object axis to the helix axis, it is apparent that $B_{a[y]}$ is proportional to a ratio of the angle bisector $B_{b[y]}/B_{b[x]}$ times the $B_{a[x]}$ value:

$$B_{a[y]} = \frac{B_{b[y]}B_{a[x]}}{B_{b[x]}} \quad (22)$$

Having computed all of B_a , the remaining intrinsic properties are easily calculated:

$$r = \|B - B_a\| \quad (23)$$

$$\theta = 2 \arcsin \frac{c}{2r} \quad (24)$$

5.6 Comparison to Screw Theory

The full version of this paper[14] provides an exposition of how to compute the same parameters using screw theory. The interactive software computes the parameters using both methods and compares the results as a test. Although roughly equivalent, the method given here is more direct. Modern computer algebra systems such as Mathematica[15] it might be possible to use these “algorithms” to produce closed-form expressions of closed-form (algebraic) inputs. For example, the Platonic solids all have lengths and face normals which can be specified exactly in closed (though irrational) form. Thus in the future it might be possible to produce a closed-form expression for the radius of one of the Platonic Dodecahelices of unit edge length, which would be harder to do from screw theory. Because this section has given analytical expressions, it is reasonable to compute the derivative of these parameters in terms of changes to basic module shape analytically. This would allow a robot made of modules to conform to a desired shape, such as maximum extent or maximum coiling, with a single change made to each module.

6 The Joint Face Normal Method

PointAxis takes a point A known to be in a specific, balanced relation to B, C and D . A chemist might know four such points from crystallography and be able to move them into this symmetric position along the z -axis.

However, one might instead know something of the subunits and how they are conjoined, without actually knowing where points A and D are.

Take as given these intrinsic properties of an object, and additionally the rule for how objects are laid face-to-face. That is, knowing the length between two joint points and a vector normal to the faces of the two joints, we almost have enough to determine the unique stacking of objects. The final piece needed is the *twist*. When face A of a second objects is placed on face B of a first object so that they are flush (that is, their normals are in opposite directions), it remains the case that the second object can be rotated about the normals. To define the joining rule, attach an *up vector* to each object, or more appropriately since we are dealing with a helix, an *out vector* that points away from the axis. Then a joining rule is “place the second object against the first, joint point coincident to joint point, and twist it so that its out vector differs by τ degrees from the out vector of the first object.” In this definition, the out vectors are considered to be measured against the plane containing the two axes meeting in a joint.

Define the *joint plane* to be the plane which contains the two faces meeting in a joint. Define the *joint line* to be the line through the joint perpendicular to the joint plane. Define the *joint angle* to be the angle of the first axis to the second measured about the joint line. The twist τ is the change in the a vector attached to the object rotated about the joint line by the joint angle. That is, take any vector attached to the first object, place it at the joint, rotate it about the joint line via the joint angle. τ is the difference between the angle of this vector measured against the joint plane and the angle of the out vector of the second object measured against the joint plane.

If the objects are macroscopic objects which have faces, this is the same as the rotation of the axis of the second object relative to the first in the plane of the coincident faces. Define intrinsic properties:

- Given an object with two identified faces, labeled B and C , assume there are normalized vectors \vec{N}_B and \vec{N}_C from each of these points that are aligned with the axis of the conjoined object attached to that face. These normals might be enforced by the fact that flat faces are joined in the joint plane. However, molecules don't have faces; this conjoining relationship may be enforced some other way.
- The length L of an object, measured from joint point A to joint point B .
- A joint twist τ defining the change in computed out-vector between objects, measured at the joint face.

For computer programmers with a graphics library supporting transformation matrices such as THREE.js[16], it is relatively easy to code the math to adjoin objects face-to-face based on the face normals, simulating the physical act of matching flat faces between macroscopic objects.

7 Changing τ Smoothly Changes Tightness

Upon implementing our interactive ability to vary τ , the following theorem becomes visually apparent.

Theorem 2 (Twist Spectrum). *For any choice of non-parallel face normals having non-zero x or y components, changing the twist angle τ through a complete rotation ($0 \leq \tau \leq 2\pi$) smoothly varies the segmented helix between a torus and flat cases.*

A proof is provided in the full version of this paper[14]. The Twist Spectrum theorem asserts that if the twist between the modules of a robot can be varied consistently, then the robot can easily move through a toroid-like shape into a linear shape and back. If it does not self-collide, it can even change the chirality or handedness of the helix it forms.

In the calculator page the τ that produces the minimum tightness (torus-like) and maximum tightness (zig-zag) to the nearest 360-degree is numerically calculated, with the labels *Minimum Tightness τ* and *Maximum Tightness τ* .

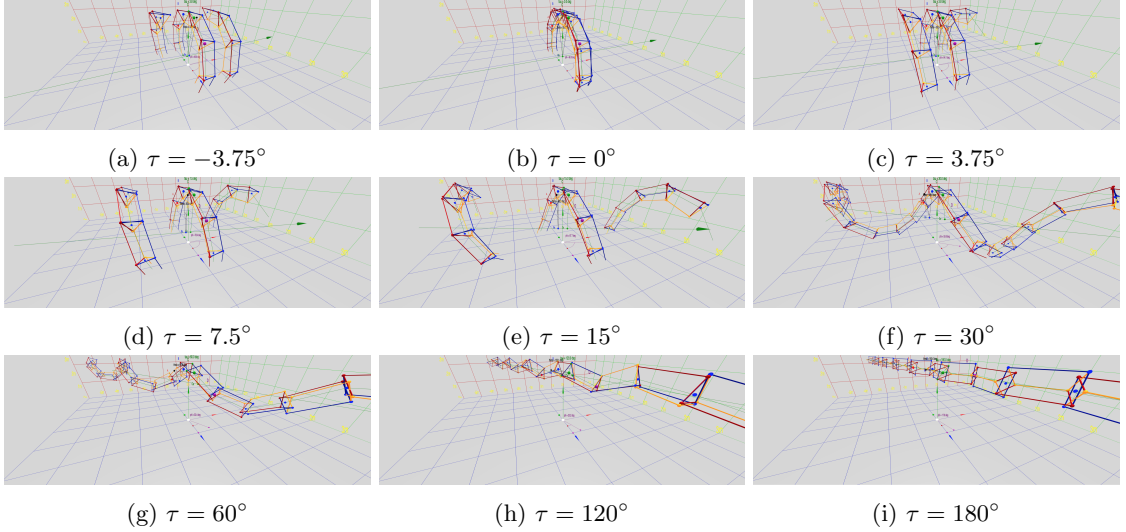
When the joint face normals are coplanar vectors, then the minimum tightness τ is always 0, and the maximum tightness occurs when $\tau = \pm\pi$. These values deviate from 0 and π roughly in proportion to the non-coplanarity of the normals.

Varying τ smoothly varies the tightness of the coiling of the helix, moving through very linear cases towards a torus, to a torus, to a very linear case on the other side.

In fact it is possible that there is always a “tightest coil” which does not self-intersect. If we had many objects, they could be packed into a convenient space by computing the τ of the tightest non-self-intersecting coil and stacking them this way. If τ can be changed, perhaps via motors in a robot arm, the object stack smoothly telescopes and contracts forming a linear actuator. A repeated molecular subunit that changed shape in response to an external magnetic or electric field or chemicals in the surrounding environment would be a telescoping nanomachine or nanoactuator.

7.1 Implications

One of the implications of having an easily-calculable understanding of the math is that it may be possible to design helices of any radius and pitch by designing periodic (possibly

Fig. 5: Coiling via change to τ

irregular) objects. Combined with slight irregularities, this means there exists a basis to design molecular helices out of “atoms” which correspond to our objects.

A modular robot constructed out of repetitions of the same shape-changing module will always produce a helix whose precise shape can be controlled by uniformly changing the shape of all of the modules. Such a robot might change its shape radically from a toroid to a linear extension.

8 Applying to The Boerdijk-Coxeter Tetrahelix

The *tetrobot*[17,18,19,20,?] is the concept of completely modular robot built entirely out of tetrahedra whose side lengths can be varied under electronic control. Such robots tend to be inherently tensegrities[21,22,23], although where the cable lengths have shrunk to zero. The current work was instigated by the author’s research with seven-tet tetrobot 1b. In particular, it is possible to construct a tentacle or snake-like or variable-geometry truss configuration of tetrahedra which, in its relaxed mode, is a regular tetrahelix.

The Boerdijk-Coxeter tetrahelix (BC helix) (see Figure 1a) is a periodic chain of conjoined regular tetrahedra which has been much studied[9,10,11,12] and happens to have irrational measures, making it an ideal test case for these algorithms. Because the face-normals can be calculated and the positions of the elements of the BC helix directly calculated, we can use it to test the algorithms, and in fact these algorithms give the same rotation.

However, it should be cautioned that the helix which Coxeter identified[9] goes through every node of every tetrahedron. Constructing the helix going through only “rail” nodes allows irregular tetrahelices to be designed[12] (see Figure 1a). However, the segmented helices defined in this paper do neither; rather, it is most natural to imagine them moving through the centroid of a face of a tetrahedron. This is a segmented helix of very small radius (0.0943) compared to the other two approaches ($\frac{3\sqrt{3}}{10} \approx 0.5196$) which measure the radius to the vertex of the tetrahedron, but it has the advantage that it is far more general. For example, it is

clearly defined if one used truncated tetrahedra. The rotation of a segment matches the BC helix analytical solution ($\theta = \arctan -3/2 \approx 131.810$), because a screw transformation does not depend on selecting a point for the radius.

8.1 Confirming Periodic Twists

The Boerdijk-Coxeter tetrahelix has an irrational rotation about the angle, meaning that is aperiodic. There is no number of perfectly regular tetrahedra that can be joined to get back to exactly the same position. A recent paper by Sadler, Fang, Clawon and Irwin[10] has explored this and given an explicit formula for a *twist* exactly as defined in this paper in order to produce a periodic tetrahelix. They explain how to compute a twist that gives a period of, for example, seven tetrahedra ($\approx 80.43^\circ$). It is gratifying that this angle does in fact produce a period-7 tetrahelix as shown in Figure ?? produced from the interactive software described herein.

In order to demonstrate the utility of the calculations explained in this paper, periodic chains of the five regular Platonic solids joined face-to-face so that their vertices coincide, which form *Platonic helices*, are explored. Such tetrahelices, icosahelices, octahelices and dodecahelices have been mentioned in a number of papers[24,25,26], but not exhaustively studied in the purely helical form. Because in some cases Platonic segmented helices may be found in nature or related to structures found in nature[27,13], our longer paper[14] has calculated all such platonic helices (there are 28 unique ones) and given their parameters in a table, the first such description of this “zoo” of structures.

9 Acknowledgements

Thanks to Prof. Eric Lord for his direct communication. The enthusiasm of the participants of the 2018 Public Invention Mathathon initiated this work.

References

1. Eric A Lord. Helical structures: the geometry of protein helices and nanotubes. *Structural Chemistry*, 13(3-4):305–314, 2002.
2. Jens Wittenburg. *Kinematics: theory and applications*. Springer, 2016.
3. Peter C Kahn. Defining the axis of a helix. *Computers & chemistry*, 13(3):185–189, 1989.
4. Robert L. Read. Segmented helix javascript code. https://github.com/PubInv/segmented-helix/blob/master/js/segment_helix_math.js, 2019.
5. Robert L. Read. Segmented helix interactive 3d calculator. <https://pubinv.github.io/segmented-helixes/index.html>, 2019.
6. Robert L. Read. The story of a public, cooperative mathathon, December 2019. [Online; posted 12-December-2019].
7. Purevjav Enkhbayar, Sodov Damdinsuren, Mitsuru Osaki, and Norio Matsushima. Helfit: Helix fitting by a total least squares method. *Computational biology and chemistry*, 32(4):307–310, 2008.
8. Hui Sun Lee, Jiwon Choi, and Sukjoon Yoon. Qhelix: a computational tool for the improved measurement of inter-helical angles in proteins. *The protein journal*, 26(8):556–561, 2007.
9. HSM Coxeter et al. The simplicial helix and the equation $\tan(n \theta) = n \tan(\theta)$. *Canad. Math. Bull.*, 28(4):385–393, 1985.

10. Garrett Sadler, Fang Fang, Richard Clawson, and Klee Irwin. Periodic modification of the boerdijk–coxeter helix (tetrahelix). *Mathematics*, 7(10):1001, 2019.
11. R.B. Fuller and E.J. Applewhite. *Synergetics: explorations in the geometry of thinking*. Macmillan, 1982.
12. Robert L. Read. Transforming optimal tetrahelices between the boerdijk–coxeter helix and a planar-faced tetrahelix. *Journal of Mechanisms and Robotics*, June 2018.
13. Peter Pearce. *Structure in Nature is a Strategy for Design*. MIT press, 1990.
14. Robert L. Read. Calculating the segmented helix formed by repetitions of identical subunits thereby generating a zoo of platonic helices. <https://github.com/PubInv/segmented-helices/blob/master/doc/StackingHelix.pdf>, 2017.
15. Wolfram Research, Inc. Mathematica, Version 12.0. Champaign, IL, 2019.
16. Jos Dirksen. *Learning Three.js: the JavaScript 3D library for WebGL*. Packt Publishing Ltd, 2013.
17. Arthur C Sanderson. Modular robotics: Design and examples. In *Emerging Technologies and Factory Automation, 1996. EFTA'96. Proceedings., 1996 IEEE Conference on*, volume 2, pages 460–466. IEEE, 1996.
18. G. J. Hamlin and A. C. Sanderson. A novel concentric multilink spherical joint with parallel robotics applications. In *Proceedings of the 1994 IEEE International Conference on Robotics and Automation*, pages 1267–1272 vol.2, May 1994.
19. Woo Ho Lee and Arthur C Sanderson. Dynamics and distributed control of tetrobot modular robots. In *Robotics and Automation, 1999. Proceedings. 1999 IEEE International Conference on*, volume 4, pages 2704–2710. IEEE, 1999.
20. Gregory J. Hamlin and Arthur C. Sanderson. *Tetrobot: A Modular Approach to Reconfigurable Parallel Robotics*. Springer Science & Business Media, 2013.
21. Brian T. Mirletz, In-Won Park, Thomas E. Flemons, Adrian K. Agogino, Roger D. Quinn, and Vytas SunSpiral. Design and control of modular spine-like tensegrity structures. In *World Conference of the International Association for Structural Control and Monitoring (IACSM)*. IACSM, July 2014.
22. NTRT - NASA Tensegrity Robotics Toolkit. <https://ti.arc.nasa.gov/tech/asr/intelligent-robotics/tensegrity/ntrt/>, 2016. Accessed: 2016-09-13.
23. Chandan Paul, Francisco J. Valero-Cuevas, and Hod Lipson. Design and control of tensegrity robots for locomotion. *IEEE Transactions on Robotics*, 22(5):944–957, 10 2006.
24. Michael Elgersma and Stan Wagon. The quadrahlenix: A nearly perfect loop of tetrahedra. *arXiv preprint arXiv:1610.00280*, 2016.
25. Hassan Babiker and Stanisław Janeczko. *Combinatorial cycles of tetrahedral chains*. IM PAN, 2012.
26. EA Lord and S Ranganathan. Sphere packing, helices and the polytope {3, 3, 5}. *The European Physical Journal D-Atomic, Molecular, Optical and Plasma Physics*, 15(3):335–343, 2001.
27. EA Lord and S Ranganathan. The γ -brass structure and the Boerdijk–Coxeter helix. *Journal of non-crystalline solids*, 334:121–125, 2004.